DALTON
FULLPAPER

Spectroscopic (UV/VIS, resonance Raman) and spectroelectrochemical study of platinum(II) complexes with 2,2′-bipyridine and aromatic thiolate ligands †

Julia A. Weinstein,*[a] Natalia N. Zheligovskaya,[a] Michael Ya. Mel'nikov[a] and František Hartl*[b]

[a] *Department of Chemistry, Moscow State University, Moscow 199899, Russia*
[b] *Anorganisch Chemisch Laboratorium, Institute of Molecular Chemistry, Universiteit van Amsterdam, Nieuwe Achtergracht 166, 1018 WV Amsterdam, The Netherlands*

A series of complexes [Pt(bpy)(4-$XC_6H_4S)_2$] (bpy = 2,2′-bipyridine; X = NO_2, H, MeO or Me_2N) have been synthesized and characterised spectroscopically. All absorb moderately in the visible region; the molar absorption coefficients of the solvatochromic absorption band lie below the values for the corresponding dithiolate complexes, indicating a slightly distorted planar geometry and a smaller HOMO − LUMO overlap. Resonance Raman, cyclic voltammetric and UV/VIS spectroelectrochemical experiments were carried out to confirm the charge transfer-to-diimine character of the visible electronic transition(s) directed from a p(S)–π(Ph)/d(Pt) delocalised orbital manifold to the π_1* LUMO of the 2,2′-bipyridine ligand. Consistent with this bonding situation: (*i*) the reduction of [Pt(bpy)(4-$XC_6H_4S)_2$] is initially localised on the bpy ligand; for X = NO_2 the second and third added electrons enter the vacant π* orbitals on the 4-NO_2 substituents; (*ii*) the resonance Raman spectra of [Pt(bpy)(4-$MeOC_6H_4S)_2$] show, besides the internal bpy modes, only a weak effect for intrathiolate (Ph–S) and ν(Pt–S) vibrations; and (*iii*) the oxidation is initially a *one-electron* process due to electronic interaction of the thiolate ligands through the platinum centre. The strongly thiolate-dependent oxidation potentials indicate a prevailing thiolate character of the HOMO.

Transition-metal diimine complexes have been intensively investigated over the past two decades as prospective objects for vectorial energy/electron transfer,[1] which may be incorporated as building blocks in molecular wires and switches. Among others, square-planar platinum(II) diimine complexes with a variety of anionic, in particular organic dithiolate, donor ligands have attracted considerable attention in this respect.[2,3] A general requirement for this kind of application is the existence of a long-lived charge-separated excited state of the metallo-organic chromophore; its stabilisation is, therefore, a problem of great interest. One of the possible solutions is to prevent rapid back electron transfer by introducing a large energy barrier which results from facile structural reorganisation following the primary interligand photoelectron transfer in mixed-ligand complexes. Platinum(II) diimine bis(thiolate) derivatives seem to be promising objects for this strategy as their charge-transfer excited states are stable towards dissociation ‡,[3h] and structural reorganisation probably occurs in the excited state at the thiolate site of the complex, involving formation of a three-electron $\overline{S–Pt–S}$ bond.[4]

The description of the low-energy excited states of this class of complexes requires first the assignment of their frontier orbitals, in particular the HOMO and LUMO. In general, several close-lying excited states of different nature can be expected within the excited-state manifolds of transition-metal complexes, in particular those complexes with mixed donor and acceptor ligands.[1a,5] For platinum(II) diimine complexes with bidentate dithiolate ligands the lowest excited state has been assigned[3e] as charge transfer to diimine by nature, with the HOMO of mixed S(p)–Pt(d) and the LUMO of diimine(π*) character. The question has arisen whether the same bonding situation, in particular with regard to the HOMO parentage, applies to their bis(thiolate) derivatives. It should be noted that for [Pt(dpphen)(4-$XC_6H_4S)_2$] (dpphen = 4,7-diphenyl-1,10-phenanthroline; X = MeO or NH_2) the parentages of the frontier orbitals have been suggested[3g] to correspond to those of platinum(II) diimine complexes containing dithiolate ligands.

The nature of the frontier orbitals involved in the photoelectron transfer process can often be elucidated by application of electrochemical and spectroelectrochemical methods.[6,7] To our knowledge no detailed (spectro)electrochemical investigation of platinum(II) diimine complexes with aromatic thiolate ligands has been carried out. In this paper we present the results of a (spectro)electrochemical study of a series of complexes [Pt(bpy)(4-XC_6H_4S)] (bpy = 2,2′-bipyridine; X = NO_2, H, MeO or Me_2N). Systematic variation of the electron-withdrawing/releasing properties of the thiolate substituent X enabled us to obtain strong evidence for a dominant contribution of the thiolate ligands to the HOMO of the complexes.

Experimental

Materials

The solvents tetrahydrofuran (thf; Acros Chimica) and dimethylformamide (dmf; Acros Chimica) were freshly distilled under a dry nitrogen atmosphere from a sodium–benzophenone mixture and calcium hydride, respectively. 4-Nitrobenzenethiol (Aldrich) was recrystallised from absolute ethanol, benzenethiol (Aldrich) and 4-methoxybenzenethiol were used as received, and 4-dimethylaminobenzenethiol was synthesized according to a literature method.[8] Hexamethylenetetraammine (urotropine) (hmt; Kazan′ Chemical Pharmaceutical Factory) was used as received. A modified literature procedure[9] was employed to synthesize [Pt(bpy)Cl_2] from $K_2[PtCl_4]$ and 2,2′-

† *Non-SI unit employed*: eV ≈ 1.60×10^{-19} J.

‡ No thiolate-radical formation was registered under 308 and 532 nm laser excitation of deaerated dmf solutions of [Pt(bpy)(4-$XC_6H_4S)_2$] (X = MeO or Me_2N), in contrast to the 365 nm, LLCT excitation of the corresponding complexes [Zn(phen)(4-$XC_6H_4S)_2$] producing the 4-XC_6H_4S radicals, detected with time-resolved UV/VIS absorption spectroscopy and as thiophenoxyl adducts with the 2-methyl-2-nitrosopropane (mnp) spin trap [see ref. 3(*i*)].

bipyridine (Aldrich). For the (spectro)electrochemical experiments PhSH, 4-$O_2NC_6H_4SH$ (both Fluka), 4-$MeOC_6H_4SH$ (Aldrich), ferrocene (BDH) and cobaltocenium hexafluorophosphate (Aldrich) were used as received. The supporting electrolyte NBu_4PF_6 (Aldrich) was recrystallised twice from absolute ethanol and dried *in vacuo* at 80 °C for 10 h.

Methods and instrumentation

Electronic absorption spectra were recorded on Shimadzu UV-2401 or software-updated Perkin-Elmer Lambda 5 spectrophotometers, ^{1}H NMR spectra on a Varian VXR-400 spectrometer. Resonance Raman measurements were performed using a Dilor Modular XY spectrometer which employs a backscattering geometry and a CCD detection system. Spinning KNO_3 pellets (214 mg KNO_3 + 18.5 mg platinum complex) at room temperature were excited at 457.9, 488.0 and 514.5 nm using lines obtained from an SP model 2016 Ar^+ laser. The incident laser power was varied between 20 and 30 mW.

The spectroelectrochemical samples were carefully prepared under an atmosphere of dry nitrogen or argon, using Schlenk techniques. The UV/VIS spectroelectrochemical experiments were carried out with an optically transparent thin-layer electrochemical (OTTLE) cell[10] (0.2 mm optical pathlength) equipped with a platinum minigrid electrode and quartz windows. The solutions were typically 3×10^{-1} M in supporting electrolyte and 2×10^{-3} M in [Pt(bpy)(4-$XC_6H_4S)_2$] or 4-$O_2NC_6H_4SH$. The potential control at the working electrode was achieved by a PA4 (EKOM) potentiostat. A thin-layer cyclic voltammogram was recorded during each potential scan at $\nu = 2$ mV s^{-1}. Bulk electrolyses of 4-XC_6H_4SH (X = H, NO_2 or MeO) to produce the corresponding thiolate anions were carried out in a gas-tight cell with a platinum flag (120 mm^2) working electrode in the middle compartment separated at the bottom by S4 frits from two lateral compartments containing platinum-gauze auxiliary and SCE reference electrodes, respectively. Conventional cyclic voltammetry was performed with an EG&G PAR model 283 potentiostat, using a gas-tight single-compartment cell equipped with platinum-disc (0.49 mm^2) working, platinum-gauze auxiliary and silver-wire pseudo-reference electrodes. The disc was repeatedly polished with a 0.25 μm grain diamond paste (PRAMET, Czech Republic). The cell contained thf solutions of 3×10^{-1} M NBu_4PF_6 and 10^{-3} M [Pt(bpy)(4-$XC_6H_4S)_2$] or reduced [4-$XC_6H_4S]^-$. The redox potentials are reported against the standard[11] ferrocene–ferrocenium couple used as an internal reference: $E_{\frac{1}{2}} = 0.575$ V *vs.* SCE in thf. For [Pt(bpy)(4-$MeOC_6H_4S)_2$] the cobaltocene–cobaltocenium redox couple served as the internal reference standard:[12] $E_{\frac{1}{2}} = -1.34$ V *vs.* ferrocene–ferrocenium.

Syntheses of [Pt(bpy)(4-$XC_6H_4S)_2$] (X = H, NO_2, MeO or Me_2N)

All these complexes were prepared from [Pt(bpy)Cl_2]. Hexamethylenetetraammine was employed as a specific 'catalyst' for the inner-sphere substitution of the chloride ligands[13] by [4-$XC_6H_4S]^-$. The products were characterised by ^{1}H NMR and UV/VIS spectroscopy, elemental analysis and molar conductivity.

[Pt(bpy)(PhS)$_2$]. A solution of hmt (280 mg, 2 mmol) in EtOH (15 cm^3) was added to a suspension of [Pt(bpy)Cl_2] (422 mg, 1 mmol) in EtOH (100 cm^3). In a separate flask PhSH (264 mg, 2.4 mmol) was added to an ethanolic solution of KBu^t (2.4 mmol in 20 cm^3) under an argon atmosphere. The resulting solution of $[PhS]^-$ was then slowly cannulated into the suspension of [Pt(bpy)Cl_2]. The reaction mixture was heated for 2 h on a water-bath with continuous stirring and bubbling with argon. The addition of the thiol solution resulted in a deep red precipitate of [Pt(bpy)(PhS)$_2$] which was filtered off, washed three times with hot water, twice with ethanol and dried under vacuum. The product, obtained in 85% yield, was used without further purification. ^{1}H NMR [$(CD_3)_2SO$]: δ 9.64 (d, *J* 5.60, 2 H), 8.66 (d, *J* 8.23, 2 H), 8.37 (t, *J* 8.00, 2 H), 7.79 (t, *J* 6.45, 2 H), 7.48 (d, *J* 7.88, 4 H), 6.91 (t, *J* 7.45, 4 H) and 6.80 (t, *J* 7.22 Hz, 2 H) (Found: C, 46.58; H, 3.19; N, 4.60. Calc. for $C_{22}H_{18}N_2PtS_2$: C, 46.41; H, 3.16; N, 4.92%).

[Pt(bpy)(4-$MeOC_6H_4S)_2$]. This was prepared using the same procedure as for [Pt(bpy)(PhS)$_2$], except that any heating had to be avoided to prevent the secondary elimination of 2,2′-bipyridine. The reaction time required to complete the coordination of [4-$MeOC_6H_4S]^-$ was 30 min at room temperature. The resulting dark red [Pt(bpy)(4-$MeOC_6H_4S)_2$] precipitate was recrystallised from acetone to remove the insoluble [Pt(4-$MeOC_6H_4S)_2$] side product. Yield 85%. ^{1}H NMR [$(CD_3)_2SO$]: δ 9.64 (d, *J* 5.70, 2 H), 8.62 (d, *J* 7.90, 2 H), 8.35 (t, *J* 7.88, 2 H), 7.77 (t, *J* 6.45, 2 H), 7.35 (d, *J* 8.88, 4 H), 6.54 (d, *J* 8.88 Hz, 4 H) and 3.60 (s, 6 H) (Found: C, 45.74; H, 3.44; N, 4.50. Calc. for $C_{24}H_{22}N_2O_2PtS_2$: C, 45.78; H, 3.50; N, 4.45%).

[Pt(bpy)(4-$Me_2NC_6H_4S)_2$]. The dark red complex was prepared using the same procedure as for [Pt(bpy)(4-MeO-$C_6H_4S)_2$]. Yield 80%. ^{1}H NMR [$(CD_3)_2SO$]: δ 9.67 (d, *J* 5.60, 2 H), 8.60 (d, *J* 8.00, 2 H), 8.32 (t, *J* 8.00, 2 H), 7.74 (t, *J* 6.36, 2 H), 7.29 (d, *J* 8.80, 4 H), 6.40 (d, *J* 8.80 Hz, 4 H) and 2.73 (s, 12 H) (Found: C, 47.62; H, 4.34; N, 8.56. Calc. for $C_{26}H_{28}N_4PtS_2$: C, 47.66; H, 4.27; N, 8.54%).

[Pt(bpy)(4-$O_2NC_6H_4S)_2$]. The bright orange complex was prepared using the same procedure as for [Pt(bpy)(PhS)$_2$], except that heating was not necessary. The substitution of the chloride ligands in [Pt(bpy)Cl_2] was completed during 30 min at room temperature. Yield 85%. ^{1}H NMR [$(CD_3)_2SO$]: δ 9.47 (d, *J* 5.90, 2 H), 8.73 (d, *J* 7.70, 2 H), 8.44 (t, *J* 7.70, 2 H), 7.86 (t, *J* 6.80, 2 H), 7.78 (d, *J* 9.35, 4 H) and 7.70 (d, *J* 8.50 Hz, 4 H) (Found: C, 40.10; H, 2.45; N, 8.33. Calc. for $C_{22}H_{16}N_2O_4PtS_2$: C, 40.08; H, 2.43; N, 8.49%).

All the complexes [Pt(bpy)(4-$XC_6H_4S)_2$] are non-electrolytes, as was demonstrated by the measured molar conductivities of 6.0–8.0 S cm^2 mol^{-1}. They are stable in the solid state and photostable in deaerated dmf solutions on irradiation at wavelengths longer than 365 nm. In air-saturated acetonitrile, dmf or dmso solutions the complexes thermally decompose within several hours at room temperature into yellow [Pt(solv)$_2$(4-$XC_6H_4S)_2$] detectable by HPLC. The formation of uncoordinated 2,2′-bipyridine in $(CD_3)_2SO$ was followed by ^{1}H NMR spectroscopy: δ 8.68 (d, H^1, 2 H), 8.38 (d, H^4, 2 H), 7.94 (t, H^3, 2 H) and 7.45 (t, H^2, 2 H). The secondary reaction (1)

$$[Pt(bpy)(4\text{-}XC_6H_4S)_2] \longrightarrow [Pt(solv)_2(4\text{-}XC_6H_4S)_2] + bpy \quad (1)$$

becomes facilitated with increasing σ-donor ability of the thiolate ligands in the order X = H < MeO < Me_2N, in accord with the stronger thiolate *trans* effect which labilises the Pt–N bonds and results in the complete elimination of the 2,2′-bipyridine ligand. Argon-saturated solutions of the complexes remain stable at room temperature for several hours. The elimination of 2,2′-bipyridine becomes, however, strongly accelerated on elevating the temperature. Warming a solution of [Pt(bpy)(4-$MeOC_6H_4S)_2$] in ethanol or dmf under argon results in rapid precipitation of the insoluble yellow complex [Pt-(4-$MeOC_6H_4S)_2$] according to equation (2) as was shown by

$$[Pt(solv)_2(4\text{-}XC_6H_4S)_2] \longrightarrow [Pt(4\text{-}XC_6H_4S)_2]\ (\text{insoluble}) \quad (2)$$

elemental analysis of the precipitate. No decomposition was observed on the timescale of hours in thf. This solvent, therefore, was chosen for the (spectro)electrochemical experiments. Complexes in chlorinated solvents exposed to daylight can decompose, probably by a slow photochemical oxidation as reported[3b,f,14] for related platinum(II) dithiolate complexes.

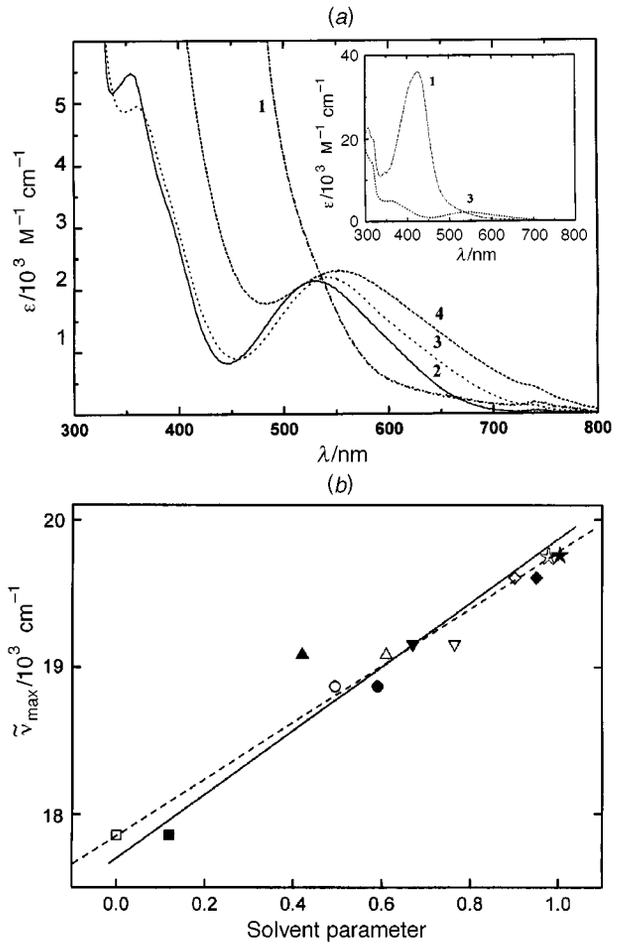

Fig. 1 (*a*) Electronic absorption spectra of 5×10^{-5} M [Pt(bpy)(4-$XC_6H_4S)_2$] in thf at 293 K. X = NO_2 (1, –·–·), H (2, ——), MeO (3, -----) or Me_2N (4, – – –). (*b*) Correlation between the charge-transfer (CT) absorption energy (E_{abs}, in cm^{-1}) of [Pt(bpy)(4-$MeOC_6H_4S)_2$] in the visible region and the unitless empirical solvent parameters *Pt*(*SS*)(*NN*)[3e] (open symbols) and E^*_{MLCT}[15] (solid symbols). Solvents used [E_{abs}, *Pt*(*SS*)(*NN*), E^*_{MLCT}]: ■, CCl_4 (17 857, 0, 0.12); ●, thf (18 868, 0.494, 0.59); ▲, $CHCl_3$ (19 084, 0.610, 0.42); ▼, CH_2Cl_2 (19 157, 0.765, 0.67); ◆, dmf (19 608, 0.901, 0.95); ★, dmso (19 763, 0.973, 1.00); linear approximation (least-squares analysis) fitted to *Pt*(*SS*)(*NN*), dashed line (slope δ = 1898 cm^{-1} = 0.23 eV; r^2 = 99.2%), and E^*_{MLCT}, solid line (slope δ = 1931 cm^{-1} = 0.24 eV; r^2 = 94.4%)

Results

Electronic absorption spectra

The electronic absorption spectra of the [Pt(bpy)(4-$XC_6H_4S)_2$] complexes exhibit in the visible region an asymmetric absorption band of medium intensity, centred at 500–540 nm in dmf and at 520–570 nm in thf [see Table 1 and Fig. 1(*a*)]. For X = NO_2 this band is obscured by the intense π ⟶ π*(NO_2) absorption. Increasing the σ,π-donor capacity of the thiolate ligands by use of more electron-releasing substituents X shifts the visible band to a lower energy and enhances the shoulder on the low-energy side. Obviously, at least two electronic transitions are hidden under the band envelope. It is noteworthy that a similar solvent-dependent asymmetric band shape was observed for [Pt(dmbpy)($PhS)_2$] (dmbpy = 4,4′-dimethyl-2,2′-bipyridine).[3f] All [Pt(bpy)(4-$XC_6H_4S)_2$] complexes show a negative solvatochromism of their absorption maxima, which correlates well with Manuta and Lees' E^*_{MLCT} {based on [$W(CO)_4$(bpy)]} and Cummings and Eisenberg's solvent scales {based on [Pt(dbbpy)(tdt)] (dbbpy = 4,4′-di-*tert*-butyl-2,2′-bipyridine, tdt = toluene-3,4-dithiolate)}[3e] [see Fig. 1(*b*)]. Non-polar solvents could not be used for the solvatochromic measurements due to the negligible solubilities of [Pt(bpy)(4-$XC_6H_4S)_2$] therein. A more profound asymmetry of the visible absorption band and a small rigidochromic effect were observed for [Pt(bpy)(4-$XC_6H_4S)_2$] on lowering the temperature to 210 K and at 77 K in a 2-methyltetrahydrofuran glass, respectively. In thf, λ_{max} and the half-width of the band are independent of the complex concentration varied in the range $c_{Pt} = 10^{-5}$–5×10^{-3} M; however, the corresponding molar absorption coefficients decrease from the values reported in Table 1 for 5×10^{-5} M solutions by *ca.* 10–30% on increasing the concentration to 3×10^{-3} M. The latter feature may point to the occurrence of aggregation of [Pt(bpy)(4-$XC_6H_4S)_2$] in the ground state at higher concentrations, *e.g. via* Pt · · · Pt contacts. No such concentration effect was observed in the presence of the supporting electrolyte NBu_4PF_6.

Table 1 Electronic absorption spectra of the complexes [Pt(bpy)(4-$XC_6H_4S)_2$] (X = NO_2, H, MeO or Me_2N), unco-ordinated 4-$O_2NC_6H_4SH$, and their reduction products; all in thf[a] at 293 K, unless stated otherwise

Compound	λ_{max}/nm (ε/10^3 M^{-1} cm^{-1})
[Pt(bpy)(4-$O_2NC_6H_4S)_2$]	243 (35), 306 (18), 314 (sh), 426 (36),[b] *ca.* 510 (sh)[c]
[Pt(bpy)($PhS)_2$]	530 (2.14),[d] 337
[Pt(bpy)(4-$MeOC_6H_4S)_2$]	543 (2.20),[e] 341
[Pt(bpy)(4-$Me_2NC_6H_4S)_2$]	557 (2.30),[f] 370 (sh)
[Pt(bpy$^{\bullet-}$)(4-$O_2NC_6H_4S)_2$]$^-$	259 (29.5), 342 (11.5), 457 (42.9), 725 (sh), 798 (2.2)
[Pt(bpy$^{\bullet-}$)(4-$O_2NC_6H_4S)_2$]$^{3-}$	272 (27.5), 382 (52.0), 464 (11.1), 501 (11.7), 560 (sh), 725 (sh), 798 (2.2), >850
[Pt(bpy$^{\bullet-}$)($PhS)_2$]$^-$	271, 364, 454, 484, 706, 787
[Pt(bpy$^{\bullet-}$)(4-$Me_2NC_6H_4S)_2$]$^-$	347 (16.6), 468 (4.8), 502 (6.4), 737 (sh), 816 (1.7), >900
4-$O_2NC_6H_4SH$	225 (sh), 318 (12.7)
[4-$O_2NC_6H_4S$]$^-$	250 (7.9), 272 (7.3), 325 (sh), 495 (24.4)
[4-$^{-\bullet}O_2NC_6H_4S$]$^{2-}$	298 (8.9), 384 (13.2), 498 (1.1)

[a] The absorption coefficients of [Pt(bpy)(4-$XC_6H_4S)_2$] correspond to 5×10^{-5} M solutions (see Results). [b] At 424 nm in CH_2Cl_2, 432 nm in dmf. [c] Obscured by the intense π ⟶ π* (NO_2) band. [d] At 512 nm in CH_2Cl_2, 498 nm in dmf. [e] At 567 nm in *o*-xylene, 521 nm in CH_2Cl_2, 509 nm in dmf. [f] At 546 nm in CH_2Cl_2, 542 nm in dmf.

Resonance Raman spectra

The resonance Raman spectra of [Pt(bpy)(4-$MeOC_6H_4S)_2$] dispersed in KNO_3 were obtained with 457.9, 488 and 514.5 nm excitation into the visible absorption band of the complex. The spectra exhibit peaks at 1603, 1560, 1491, 1321, 1277, 1177, 1031 and 663 cm^{-1} which are assigned straightforwardly to the internal modes of the co-ordinated 2,2′-bipyridine.[16] The peak at 1491 cm^{-1} possesses a higher intensity relative to those at 1603 and 1560 cm^{-1}. Such an intensity pattern is characteristic of charge-transfer electronic transitions directed to the lowest empty orbital of the 2,2′-bipyridine ligand, *i.e.* π_1*(bpy).[16] In addition, very weak Raman bands were observed at 1092, 733, 642, 452, 428, 414, 395, 374 and 280 cm^{-1} which may be assigned to internal thiolate, mainly phenyl-ring[17] vibrations. The band at 374 cm^{-1} may also belong to the ν(Pt–S) or ν(Pt–N) modes expected[17,18] in this case between 320 and 380 cm^{-1}.

(Spectro)electrochemistry

The redox behaviour of the complexes [Pt(bpy)(4-$XC_6H_4S)_2$] and of selected free thiolates were studied in thf by cyclic

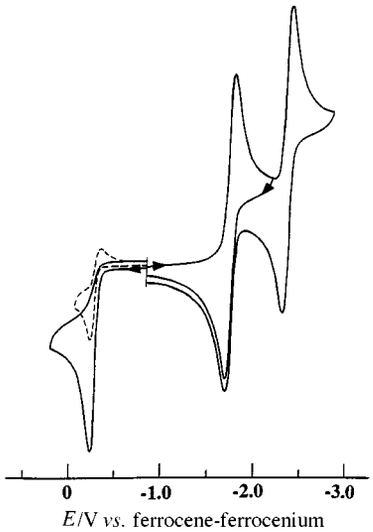

Fig. 2 Cyclic voltammogram of 10^{-3} M [Pt(bpy)(4-$Me_2NC_6H_4S)_2$]. Conditions: 10^{-3} M solution in thf–3×10^{-1} M NBu_4PF_6, 293 K, platinum-disc electrode (0.49 mm^2 apparent surface area), $\nu = 100$ mV s^{-1}. The dotted curve corresponds to the anodic scan at 210 K

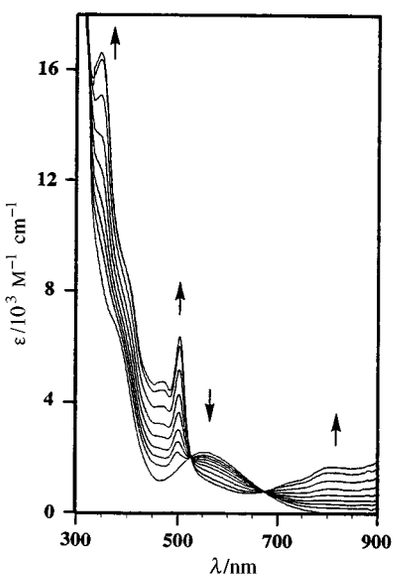

Fig. 3 The UV/VIS spectral changes accompanying the 1e reduction of [Pt(bpy)(4-$Me_2NC_6H_4S)_2$]. Conditions: 2×10^{-3} M solution in thf–3×10^{-1} M NBu_4PF_6, 293 K; electrolysis within an OTTLE cell [10]

voltammetry and UV/VIS spectroelectrochemistry. The redox potentials of the compounds are listed in Table 2.

Reduction. A typical cyclic voltammogram of [Pt(bpy)(4-$XC_6H_4S)_2$] (X = H, MeO or Me_2N) is shown for X = Me_2N in Fig. 2. All three complexes undergo chemically and electrochemically reversible one-electron reduction the half-wave potential of which slightly decreases with increasing donor capacity of the thiolate ligands. The corresponding UV/VIS spectroelectrochemical experiment established that the electron transfer from the platinum cathode is directed to the π_1*(bpy) LUMO, as judged from the appearance of the characteristic bands of $[Pt(bpy^{\bullet -})(4\text{-}Me_2NC_6H_4S)_2]^-$ at λ_{max} = 468, 502, 737 (sh) and 816 nm, together with an additional band below 900 nm (see Fig. 3), belonging to the characteristic [21] $\pi^* \longrightarrow \pi^*$ intraligand (IL) electronic transitions of the $[bpy]^{\bullet -}$ radical anion. For $[Pt(bpy^{\bullet -})(PhS)_2]^-$ these IL transitions shift to higher energies, *viz.* to λ_{max} = 454, 484, 706 and 787 nm.

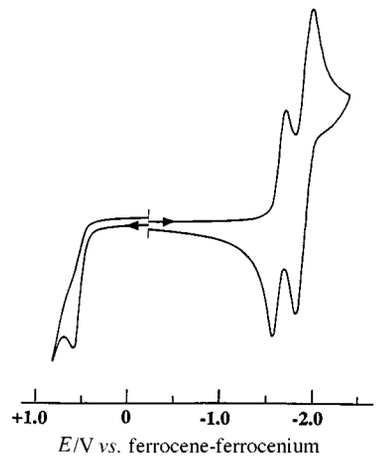

Fig. 4 Cyclic voltammogram of [Pt(bpy)(4-$O_2NC_6H_4S)_2$]. Conditions: see Fig. 2

The subsequent one-electron reduction of the radical anions producing $[Pt(bpy)(4\text{-}XC_6H_4S)_2]^{2-}$ (X = H, MeO or Me_2N) is chemically reversible on the voltammetric timescale defined by $\nu > 100$ mV s^{-1}; it is however electrochemically quasi-reversible, as indicated by the slightly larger and scan-rate dependent ΔE_p values relative to ΔE_p(ferrocene–ferrocenium) (see Table 2). During the UV/VIS spectroelectrochemical experiments at 293 K, $[Pt(bpy)(4\text{-}Me_2NC_6H_4S)]^{2-}$ was only detected as a short-lived transient absorbing in thf at *ca.* 600 nm. Its decomposition was not studied in detail. In view of the nearly invariable reduction potentials of the radical anions (see Table 2) we propose that also the second cathodic step is initially localised on the 2,2′-bipyridine ligand.

The reduction path of [Pt(bpy)(4-$O_2NC_6H_4S)_2$] is partly different due to the presence of the reducible conjugated *p*-NO_2 substituents on the thiolate ligands. The cyclic voltammogram of the latter complex exhibits a reversible one-electron cathodic process which is followed by two overlapping one-electron waves (see Table 2 and Fig. 4). The diffusion coefficient of the complex, $D_{Pt} = 3.0 \times 10^{-6}$ cm^2 s^{-1}, was determined relative to that of the internal ferrocene standard ($D_{Fc} = 8.0 \times 10^{-6}$ cm^2 s^{-1} in thf [22]), and from direct application of equation (3) where $I_{p,c}$

$$I_{p,c} = 2.69 \times 10^5 n^{\frac{3}{2}} A D^{\frac{1}{2}} \nu^{\frac{1}{2}} C \qquad (3)$$

is the peak current of the first cathodic wave, A the real surface area of the cathode and C the bulk concentration of the complex.[23]

From the voltammetric response it was not clear whether the initial one-electron step involves reduction of the 2,2′-bipyridine ligand followed by parallel one-electron reduction of both *p*-NO_2 groups, or if one of the $[4\text{-}O_2NC_6H_4S]^-$ ligands is reduced first. The latter possibility may get support from the more positive reduction potential of unco-ordinated $[4\text{-}O_2NC_6H_4S]^-$ relative to that of 2,2′-bipyridine (see Table 2). An unambiguous assignment of the electron-transfer sequence proved to be possible on the basis of the corresponding UV/VIS spectroelectrochemical information. The one-electron reduction of [Pt(bpy)(4-$O_2NC_6H_4S)_2$] led to the appearance of weak bands at 725 (sh), 798 and 850 nm attributable to the IL transitions of the co-ordinated $[bpy]^{\bullet -}$ radical anion. The other IL bands between 400 and 500 nm are obscured by the intense $\pi \longrightarrow \pi^*$ (NO_2) band of $[Pt(bpy^{\bullet -})(4\text{-}O_2NC_6H_4S)_2]^-$ at 457 nm, which had shifted to lower energy compared to that of the neutral parent complex (see Fig. 5 and Table 1). The unresolved second and third one-electron reduction steps produced the trianion $[Pt(bpy)(4\text{-}O_2NC_6H_4S)_2]^{3-}$ the UV/VIS spectrum (see Fig. 6) of which exhibits a characteristic sharp IL band of the singly reduced dianionic ligand $[4\text{-}^{-\bullet}O_2NC_6H_4S]^{2-}$ at 382 nm.

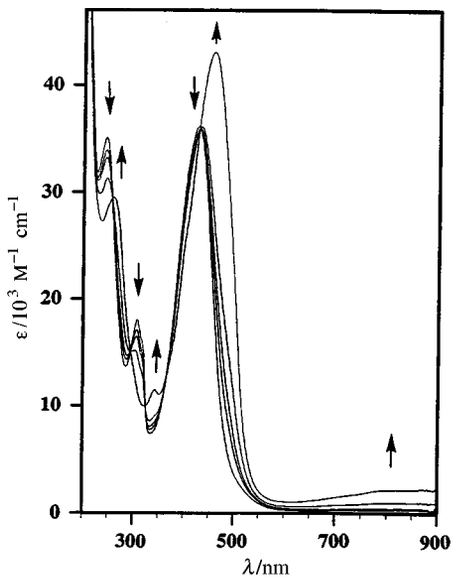

Fig. 5 The UV/VIS spectral changes accompanying the 1e reduction of $[Pt(bpy)(4\text{-}O_2NC_6H_4S)_2]$. Conditions: see Fig. 3

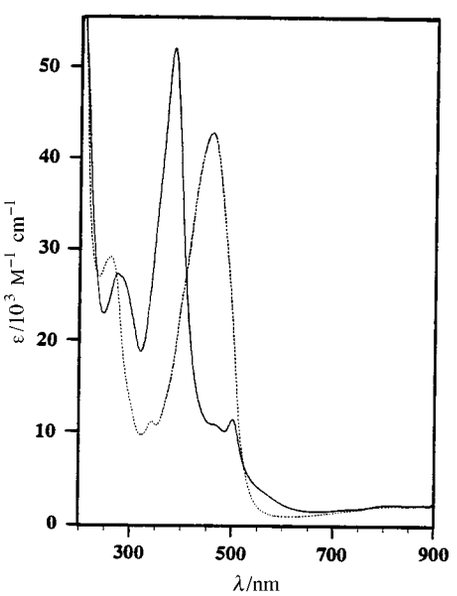

Fig. 6 The UV/VIS spectra of $[Pt(bpy^{\bullet -})(4\text{-}O_2NC_6H_4S)_2]^-$ (dotted line) and $[Pt(bpy^{\bullet -})(4\text{-}O_2NC_6H_4S)_2]^{3-}$ (solid line). The trianion was generated under conditions given in Fig. 3

This band is found at 384 nm in the UV/VIS spectrum of the unco-ordinated dianion generated on stepwise reduction of the precursor $4\text{-}O_2NC_6H_4SH$ and $[4\text{-}O_2NC_6H_4S]^-$ (see Fig. 7 and Table 1). The UV/VIS spectrum of $[Pt(bpy)(4\text{-}O_2NC_6H_4S)_2]^{3-}$ also clearly shows the characteristic $\pi^* \longrightarrow \pi^*$ IL bands of the $[bpy]^{\bullet -}$ ligand at $\lambda_{max} = 464$ and 501 nm; the lower-lying IL bands of $[bpy]^{\bullet -}$ do not change their position on the two-electron reduction of $[Pt(bpy^{\bullet -})(4\text{-}O_2NC_6H_4S)_2]^-$ (see Fig. 6).

Oxidation. Cyclic voltammetry reveals that the $[Pt(bpy)(4\text{-}XC_6H_4S)_2]$ complexes rapidly decompose during oxidation at room temperature (see Figs. 2 and 4). The oxidation potential $E_{p,a}$ shifts considerably negatively with increasing donor capacity of the thiolate ligands. Notably, the difference between the $E_{p,a}$ values for $[Pt(bpy)(4\text{-}XC_6H_4S)_2]$ is equal to or even larger than that observed in the case of the chemically irreversible oxidation of the unco-ordinated anions $[4\text{-}XC_6H_4S]^-$ (generated by preparative electrolysis of the corresponding thiophenols; see Table 2). A comparison of the cathodic and anodic peak currents due to the reduction and oxidation of $[Pt(bpy)(4\text{-}XC_6H_4S)_2]$, respectively, points to the one-electron character of the oxidation step on the timescale defined by $\nu \geqslant 100$ mV s^{-1}. Importantly, the one-electron oxidation of $[Pt(bpy)(4\text{-}Me_2NC_6H_4S)_2]$ in thf becomes partly chemically reversible on cooling to 210 K (see Fig. 2). This result sharply contrasts with the oxidation of $[Pt(bpy)(4\text{-}O_2NC_6H_4S)_2]$ which remains totally chemically irreversible at this temperature.

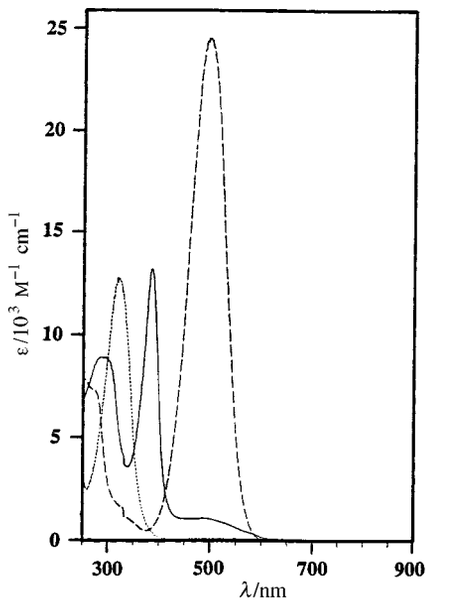

Fig. 7 The UV/VIS spectra of unco-ordinated $4\text{-}O_2NC_6H_4SH$ (dotted line) and its consecutive reduction products, the anion $[4\text{-}O_2NC_6H_4S]^-$ (dashed line) and the radical dianion $[4\text{-}^{\bullet}O_2NC_6H_4S]^{2-}$ (solid line). A spectroelectrochemical experiment under conditions given in Fig. 3

Discussion

The one-electron reduction of all the complexes $[Pt(bpy)(4\text{-}XC_6H_4S)_2]$ under study is localised on the LUMO which possesses, as could be anticipated,[3,7] an almost exclusive π_1^*(bpy) character. The gradual positive shift of $E_{\frac{1}{2}}(bpy^{0/\bullet -})$ by 180 mV on proceeding from the strongly donating thiolate ligand with $X = Me_2N$ to that with the electron-withdrawing NO_2 substituent can reasonably be ascribed to the increased bpy→Pt σ donation in the latter case. The same conclusions can be drawn for the second one-electron reduction step, with the exception of $[Pt(bpy^{\bullet -})(4\text{-}O_2NC_6H_4S)_2]^-$ which reduces at the thiolate ligands.

The comparatively large variation of the oxidation potentials of $[Pt(bpy)(4\text{-}XC_6H_4S)_2]$ and those of the corresponding free anions $[4\text{-}XC_6H_4S]^-$ as reference compounds points to a dominant thiolate character of the HOMO of the complexes. The same conclusion was made, *e.g.* for $[Pt^{II}(bpy)(\mu\text{-}S_2M^{VI}S_2)]$ (M = Mo or W)[2e] and for [Pt(bpy)L] [L = tdt or catecholate (cat)],[24] in the latter case being substantiated by a large hypsochromic shift (2000 cm^{-1}) of the lowest-energy charge-transfer band on replacing the catecholate by the more easily oxidisable tdt ligand.[25] In contrast to this assignment, Eisenberg and coworkers[3] have ascribed the HOMO of a large number of Pt(α-diimine)(dithiolate) complexes to a strongly mixed Pt(d)–S(p) orbital, and classified the HOMO ⟶ LUMO electronic transition as a 'charge transfer to diimine' process. This general term has been adopted also for platinum(II) diimine complexes with aromatic thiolate ligands, *e.g.* for $[Pt(dpphen)(4\text{-}XC_6H_4S)_2]$ (X = MeO or Me_2N).[3g]

In view of the strongly thiolate-dependent oxidation potentials of $[Pt(bpy)(4\text{-}XC_6H_4S)_2]$, the HOMO of the complexes possesses a large contribution from the p(S) and $\pi(C_6H_4X)$ orbitals, which can be even *larger* than predicted by extended Hückel (EH) calculations on the *model* complex with X = H,

Table 2 Cyclic voltammetric data of the investigated complexes [Pt(bpy)(4-$XC_6H_4S)_2$] (X = NO_2, H, MeO or Me_2N), unco-ordinated 2,2′-bipyridine, corresponding thiolate anions and thiophenols, and related [Pt(bpy)L_2] complexes; all in thf at 293 K, unless stated otherwise[a]

Compound	$E_{p,a}^{ox}$ (ΔE_p)	$E_{\frac{1}{2}}^{red\ I}$ (ΔE_p)	$E_{\frac{1}{2}}^{red\ II}$ (ΔE_p)	ΔE_p (ferrocene–ferrocenium)
[Pt(bpy)(4-$O_2NC_6H_4S)_2$]	+0.58	−1.60 (110)	−1.87[b] (140)	110
	+0.66[c]	−1.59[c] (100)	−1.83[b,c] (150)	100
[Pt(bpy)$(PhS)_2$]	+0.22	−1.72 (110)	−2.37 (130)	110
	+0.31[d]	−1.67[d] (100)	−2.33[d] (150)	100
[Pt(bpy)(4-$MeOC_6H_4S)_2$]	−0.04	−1.76 (100)	−2.39 (120)	100
[Pt(bpy)(4-$Me_2NC_6H_4S)_2$]	−0.23	−1.78 (120)	−2.41 (140)	120
	−0.21[c,e] (125)	−1.67[c] (100)	−2.30[c] (140)	100
bpy[f]		−2.72 (120)	−3.29[g,h]	120
[4-$O_2NC_6H_4S$]$^-$	−0.18	−2.08[i]		
[PhS]$^-$	−0.54			
[4-$MeOC_6H_4S$]$^-$	−0.65			
4-$O_2NC_6H_4SH$		−1.46[g–i]		
PhSH		−1.70[g,h]		
4-$MeOC_6H_4SH$		−1.80[g,h]		
[Pt(bpy)Cl_2]	+0.67	−1.64 (83)	−2.30[g]	
[Pt(bpy)$(mes)_2$][j]	+0.45[k] (60)	−2.05	−2.73	
[Pt(bpy)(tdt)][l]	−0.024[e]	−1.739		

[a] Definitions: $E_{p,a}^{ox}$ = anodic peak potential of chemically irreversible oxidation, $E_{\frac{1}{2}}^{red}$ = half-wave potential of chemically reversible reduction in V; ΔE_p = cathodic-to-anodic peak separation in mV. [b] Overall transfer of 2e; two overlapping one-electron reductions of the 4-NO_2 groups of the thiolate ligands. [c] At 210 K. [d] In dmf at 293 K. [e] Chemically partly reversible. [f] From ref. 19. [g] Chemically irreversible. [h] Cathodic peak potential. [i] Data in acetonitrile reported in ref. 20. [j] From ref. 7. [k] Chemically reversible. [l] From ref. 3(*e*).

showing strongly mixed Ph(π)–S(p)–Pt(d) characters for the closely spaced HOMO, HOMO-1 (ΔE = 0.06 eV) and HOMO-2 (ΔE = 0.22 eV).[3f] In this respect it is important to note that the EH calculations on [Pt(bpy)$(PhS)_2$] were based only on X-ray data on dithiolate complexes, *e.g.* almost planar [Pt(bpym)(mnt)] (bpym = 2,2′-bipyrimidine, mnt = maleonitriledithiolate),[26] and similar compounds, but not on any Pt(α-diimine)(thiolate)$_2$ structure which may deviate from planarity to some extent, as discussed below. Consequently, the true parentages of the occupied frontier orbitals still remain a matter of discussion, although the mixed character of the HOMO with prevailing contribution from the thiolate ligands is indisputable. We assume that the thiolate contribution to the HOMO is not constant and may vary with the donor strength of X. It is probable that in such a case a profound dependence of the oxidation potentials of [Pt(bpy)(4-$XC_6H_4S)_2$] on the donor properties of the thiolate ligands will still be observed independent of the variable HOMO parentage. For example, the HOMO of related [Pt(bpy)(edt)] (edt = ethane-1,2-dithiolate) possesses a 41% Pt and 56% edt character, whereas with the significantly more electron-withdrawing maleonitriledithiolate ligand the HOMO becomes apparently more dithiolate-localised (27% Pt/72% mnt).[3f] The Bu^t derivative [Pt(dbbpy)(edt)] then oxidises significantly more negatively than [Pt(dbbpy)(mnt)]: $\Delta E_{p,a}$ = −0.513 V.[3e] In our case the fairly strong Pt(d)–S(p)–Ph(π) mixing in the HOMO of [Pt(bpy)(4-$XC_6H_4S)_2$] is reflected in the one-electron character of the primary oxidation step, as was unambiguously confirmed for X = Me_2N at low temperatures. We can reasonably expect that the absence of electronic communication between the two thiolate ligands through the platinum would result in their nearly parallel one-electron oxidation, *i.e.* in the transfer of two electrons. Thus, the reduction of the non-interacting 4-NO_2 substituents in [Pt(bpy)-(4-$O_2NC_6H_4S)_2$] is indeed an unresolved two-electron step.

The higher stability of the one-electron oxidised complex [Pt(bpy)(4-$Me_2NC_6H_4S)_2$]$^+$ at low temperatures in comparison with the unstable cation [Pt(bpy)(4-$O_2NC_6H_4S)_2$]$^+$ corresponds with the more efficient *photooxidation* of the parent complex [Pt(bpy)(4-$O_2NC_6H_4S)_2$].[27a] In the charge-separated excited state of the latter complex probably a three-electron $\overline{S–Pt–S}$ bond[5] is formed which is stabilised by the electron-withdrawing 4-NO_2 substituent. Its presence increases sufficiently the excited-state lifetime. This allows electron transfer to the internal electron acceptor benzyl viologen (1,1′-dibenzyl-4,4′-bipyridinium) to occur.[27a] The one-electron *electrochemical* oxidation of [Pt(bpy)(4-$XC_6H_4S)_2$] is probably also followed by the formation of the aforementioned $\overline{S–Pt–S}$ bond. The energy barrier for the latter process is then probably relatively high in the presence of the donor substituent X = 4-Me_2N, which may explain the partial chemical reversibility of the one-electron oxidation of [Pt(bpy)(4-$Me_2NC_6H_4S)_2$] at low temperatures. The subsequent electron-transfer step from the $\overline{S–Pt–S}$-bound transient to the anode ultimately produces free disulfide, as was also observed during the photooxidation reactions.§

The solvent-dependent asymmetric visible absorption band of [Pt(bpy)(4-$XC_6H_4S)_2$] obviously belongs to charge-transfer electronic transitions directed to the empty π_1*(bpy) orbital, as was also confirmed by resonance Raman spectroscopy in the case of [Pt(bpy)(4-$MeOC_6H_4S)_2$]. The very weak resonance Raman effect of the internal thiolate (Ph ring) and possibly also ν(Pt–S) modes implies that the bonds within the platinum thiolate moiety are hardly affected during the electronic transition. This result again supports the rather delocalised Ph(π)–S(p)–Pt(d) bonding situation in this complex (see above). The alternative assignment of the visible absorption band to a largely Pt(d)→bpy(π_1*) charge-transfer transition can be excluded in view of the absence of a corresponding low-energy absorption band in the UV/VIS spectra of yellow [Pt(bpy)Cl_2]. The EH calculations performed[3f] on [Pt(bpy)$(PhS)_2$] indeed revealed several occupied orbitals delocalised over the Pt–SPh moiety, which lie in close proximity to each other (see above). In this respect we cannot exclude the possibility that the resonance Raman experiments with [Pt(bpy)(4-$MeOC_6H_4S)_2$] (λ_{exc} = 457.8, 488 and 514.5 nm) were performed on excitation into a visible charge transfer-to-diimine transition which originates from a strongly platinum thiolate delocalised donor orbital underlying the HOMO, *e.g.* the HOMO-2 as described for [Pt(bpy)$(PhS)_2$].[3f] Thus, matrix analysis[28] applied to a series of UV/VIS spectra of 10^{-3}–10^{-5} M [Pt(bpy)(4-$MeOC_6H_4S)_2$] in thf revealed two absorption bands centred at 530 and 630 nm, independent of concentration, which exhibit equal solvato-

§ Photooxidation of [Pt(phen)$(PhS)_2$] in air-saturated butyronitrile resulted in the appearance of the characteristic[27b] intense absorption band of unco-ordinated PhSSPh at 242 nm (ε = 1.3 × 10^4 M cm^{-1}).

chromism. As already noted, UV/VIS spectra of [Pt(dmbpy)-$(PhS)_2$] also show a broad visible absorption band with a shoulder on its long-wavelength side which becomes particularly apparent in apolar solvents[3f] and may belong to the HOMO ⟶ LUMO transition. This shoulder of the main visible band may alternatively be assigned to a spin-forbidden singlet ⟶ triplet charge transfer-to-diimine transition which has sufficient intensity due to the presence of the heavy $5d^8$ metal centre. We prefer the latter assignment which is also consistent with the charge-transfer absorption characteristics of some Pt(diimine)(dithiolate) complexes studied by Schanze and co-workers,[27] and Pt(diimine)$(mes)_2$ (mes = 2,4,6-trimethylphenyl).[7]

The relatively small molar absorption coefficients for the main visible absorption band of [Pt(bpy)$(4\text{-}XC_6H_4S)_2$] (X = H, MeO or Me_2N) ($\varepsilon_{max} \approx 2000$ M^{-1} cm^{-1}) compared to those of the corresponding dithiolate complexes (ε_{max} = 5000–15 000 M^{-1} cm^{-1})[3] are noteworthy. For [Pt(dpphen)$(4\text{-}MeOC_6H_4S)_2$] with the more rigid dpphen ligand a value ε_{max} = 3000 M^{-1} cm^{-1} was reported.[3g] In view of our results, the characteristic value $\varepsilon_{max} \geqslant 10\,000$ M^{-1} cm^{-1} measured by Eisenberg and co-workers[3f] for a series of Pt(diimine)(dithiolate) complexes is unlikely to apply to [Pt(dmbpy)$(PhS)_2$]. We may assume that the torsion angle between the 2,2′-bipyridine and thiolate ligands is slightly larger than in the case of the more rigid dithiolate ligands, for example due to the thermal excitation of torsional vibrations. In addition, rotation of the Ph rings of the thiolate ligands out of the Pt(bpy) plane might cause a poorer orbital overlap between the frontier orbitals involved in the optical electron transfer and, consequently, the lower intensity of the visible charge-transfer absorption band of [Pt(bpy)$(4\text{-}XC_6H_4S)_2$]. These arguments are indeed supported by the recently reported first crystal structure of platinum(II) diimine bis(monothiolate) complex, where diimine = dpphen and thiolate = 1,2-dicarba-*closo*-dodecaborane(12)-1-thiolate.[30]

The higher-lying absorption band of [Pt(bpy)$(4\text{-}XC_6H_4S)_2$] centred in dmf at 330–370 nm also belongs to an interligand charge-transfer electronic transition, as documented by its red shift on increasing the donor capacity of the thiolate ligands. The separation between the vacant π_1* and π_2* orbitals of co-ordinated 2,2′-bipyridine is known to vary between 7000 and 9000 cm^{-1}.[16,31] This value corresponds well to the energetic difference between the main visible band and the higher-energy one, which amounts to 9670 and 9200 cm^{-1} for [Pt(bpy)$(4\text{-}XC_6H_4S)_2$], X = H and Me_2N, respectively. The absorption band at 330–370 nm is, therefore, attributed to an electronic transition from the mixed π(Ph)–p(S)/d(Pt) orbital manifold to the π_2*(bpy) orbital.

Conclusion

The resonance Raman and (spectro)electrochemical data presented in this study suggest significant p(S)–π(Ph) and d(Pt) orbital contributions to the HOMO of [Pt(bpy)$(4\text{-}XC_6H_4S)_2$], and a dominant π_1*(bpy) contribution to the LUMO. In this respect these complexes resemble their dithiolate derivatives. Further research, in particular single-crystal X-ray studies,[30] is needed to gain evidence for the anticipated position of the thiolate Ph rings out of the Pt(bpy) plane and for a larger torsion angle between the 2,2′-bipyridine and the thiolate ligands, compared to the corresponding dithiolate complexes. These structural differences are thought to be responsible for the less intense visible charge transfer-to-diimine absorption of [Pt(bpy)$(4\text{-}XC_6H_4S)_2$] relative to the dithiolate derivatives. The X-ray data would also allow the nature of the frontier orbitals of the bis(thiolate) complexes to be calculated with higher precision. For example, density functional calculations,[6a] suitable for an unambiguous interpretation of electrochemical and UV/VIS absorption data, could be undertaken.

Acknowledgements

This work was supported by the Russian Fund of Basic Research (grant no. 96-03-32530), the Netherlands Foundation of Chemical Research (SON) and the Netherlands Organization for the Advancement of Pure Science (NWO). J. A. W. is grateful for financial support within the framework of the Exchange Agreement between the University of Amsterdam and the Moscow State University to support her stay in Amsterdam. We owe thanks to Theo L. Snoeck (University of Amsterdam) for recording the resonance Raman spectra, and to Professor Derk J. Stufkens (University of Amsterdam) and Dr. Alex Galin (Moscow State University) for valuable discussions and interest in this work.

References

1 (*a*) T. J. Meyer, in *Photochemical Processes in Organized Molecular System*, ed. K. Honda, Elsevier, Amsterdam, 1991, p. 133; (*b*) V. Balzani, S. Campagna, G. Denti, A. Juris, S. Serroni and M. Venturi, *Coord. Chem. Rev.*, 1994, **132**, 1; (*c*) K. Kalyanasundaram, *Coord. Chem. Rev.*, 1982, **46**, 159; (*d*) P. R. Auburn and A. B. P. Lever, *Inorg. Chem.*, 1990, **29**, 2551.

2 (*a*) A. Harriman and R. Ziessel, *Chem. Commun.*, 1996, 1707; (*b*) V. Grosshenny, A. Harriman, M. Hissler and R. Ziessel, *J. Chem. Soc., Faraday Trans.*, 1996, 2223; (*c*) A. Harriman, M. Hissler, R. Ziessel, A. De Cian and J. Fisher, *J. Chem. Soc., Dalton Trans.*, 1995, 4067; (*d*) P. I. Kvam, M. I. V. Puzyk, V. S. Cotlyr, J. Songstang and K. P. Balashev, *Acta Chem. Scand.*, 1996, **50**, 6; (*e*) H. Kunkely and A. Vogler, *Inorg. Chim. Acta*, 1997, **264**, 305; (*f*) S. P. Kaiwar, A. Vodachek, N. V. Blough and R. S. Pilato, *J. Am. Chem. Soc.*, 1997, **119**, 9211.

3 (*a*) J. A. Zuleta, J. Bevilacqua and R. Eisenberg, *Coord. Chem. Rev.*, 1991, **111**, 237; (*b*) J. A. Zuleta, M. S. Burberry and R. Eisenberg, *Coord. Chem. Rev.*, 1990, **97**, 47; (*c*) J. Bevilacqua and R. Eisenberg, *Inorg. Chem.*, 1994, **33**, 2913; (*d*) S. D. Cummings and R. Eisenberg, *Inorg. Chem.*, 1995, **34**, 2007; (*e*) S. D. Cummings and R. Eisenberg, *J. Am. Chem. Soc.*, 1996, **118**, 1949; (*f*) J. A. Zuleta, J. Belvilacqua, D. M. Prosperio, P. D. Harvey and R. Eisenberg, *Inorg. Chem.*, 1992, **31**, 2396; (*g*) S. D. Cummings, L.-T. Cheng and R. Eisenberg, *Chem. Mater.*, 1997, **9**, 440; (*h*) J. Weinstein, M. Mel'nikov, V. Plyusnin and V. Grivin, unpublished work; (*i*) A. M. Gallin, Yu. V. Razskazovsky and M. Ya. Mel'nikov, *J. Photochem. Photobiol. A: Chem.*, 1994, **78**, 113.

4 (*a*) K.-D. Asmus, in *Sulfur-Centered Reactive Intermediates in Chemistry and Biology*, eds. C. Chatgilialoglu and K.-D. Asmus, NATO-ASI Series, Plenum, New York, 1991 and refs. therein; (*b*) M. Gobl, M. Bonifacic and K.-D. Asmus, *J. Am. Chem. Soc.*, 1984, **106**, 5984; (*c*) D. A. Armstrong, ref. 4(*a*), pp. 121–134 and 341–351.

5 S. M. Frederics, J. C. Luong and M. S. Wrighton, *J. Am. Chem. Soc.*, 1979, **101**, 7415; M. Martin, M.-B. Krogh-Jespersen, M. Hsu, J. Tewksbury, M. Laurent, K. Viswanath and H. Patterson, *Inorg. Chem.*, 1983, **22**, 647.

6 (*a*) M. P. Aarnts, M. P. Wilms, K. Peelen, J. Fraanje, K. Goubitz, F. Hartl, D. J. Stufkens, E. J. Baerends and A. Vlček, jun., *Inorg. Chem.*, 1996, **35**, 5468; (*b*) B. D. Rossenaar, F. Hartl and D. J. Stufkens, *Inorg. Chem.*, 1996, **35**, 6194; (*c*) F. Hartl and A. Vlcek, jun., *Inorg. Chem.*, 1991, **30**, 3048.

7 A. Klein and W. Kaim, *Organometallics*, 1995, **14**, 1176.

8 A. M. Galin, Y. V. Razskazovskii and M. Ya. Mel'nikov, *Russ. J. High Energy Chem.*, 1993, **27**, 69.

9 G. T. Morgan and F. H. Burstal, *J. Chem. Soc.*, 1934, 965.

10 M. Krejčík, M. Daněk and F. Hartl, *J. Electroanal. Chem., Interfacial Electrochem.*, 1991, **313**, 243.

11 G. Gritzner and J. Kuta, *Pure Appl. Chem.*, 1984, **56**, 461.

12 R. S. Stojanovic and A. M. Bond, *Anal. Chem.*, 1993, **65**, 56.

13 N. Zheligovskaya, L. Kopaneva and E. Pomakhina, *Russ. J. Coord. Chem.*, 1995, **21**, 570.

14 A. Vogler and H. Kunkely, *J. Am. Chem. Soc.*, 1981, **103**, 1559; *Inorg. Chem.*, 1982, **21**, 1172; A. Vogler, H. Kunkely, J. Hlavatsch and A. Merz, *Inorg. Chem.*, 1984, **23**, 506; H. Kunkely and A. Vogler, *J. Am. Chem. Soc.*, 1990, **112**, 5625.

15 D. M. Manuta and A. J. Lees, *Inorg. Chem.*, 1983, **22**, 3825.

16 F. Hartl, T. L. Snoeck, D. J. Stufkens and A. B. P. Lever, *Inorg. Chem.*, 1995, **34**, 3887 and refs. therein.

17 K. Nakamoto, in *Infrared and Raman Spectra of Inorganic and Coordination Compounds*, Wiley, New York, 5th edn., 1997, part B.

18 D. J. Stufkens, T. L. Snoeck and B. J. van der Veken, *Inorg. Chim. Acta*, 1983, **76**, L253; J. R. Alkins and P. J. Hendra, *J. Chem. Soc. A*, 1967, 1325.
19 R. A. Klein, C. J. Elsevier and F. Hartl, *Organometallics*, 1997, **16**, 1284.
20 D. E. Bartak, T. M. Shields and M. D. Hawley, *J. Electroanal. Chem.*, *Interfacial Electrochem.*, 1971, **30**, 289.
21 (*a*) M. Krejčík and A. A. Vlček, *J. Electroanal. Chem.*, *Interfacial Electrochem.*, 1991, **313**, 243; (*b*) J. Víchová, F. Hartl and A. Vlcek, jun., *J. Am. Chem. Soc.*, 1992, **114**, 10 903; (*c*) B. C. Noble and R. D. Peacock, *Spectrochim. Acta*, *Part A*, 1990, **46**, 407.
22 C. Amatore, M. Azzabi, P. Calas, A. Jutand, C. Lefrou and Y. Rollin, *J. Electroanal. Chem.*, *Interfacial Electrochem.*, 1990, **288**, 45.
23 A. J. Bard and L. R. Faulkner, in *Electrochemical Methods: Fundamentals and Applications*, Wiley, New York, 1980, p. 218.
24 R. Benedix and H. Hennig, *Inorg. Chim. Acta*, 1988, **141**, 21.
25 L. Kumar, K. H. Puthraya and T. S. Shrivastava, *Inorg. Chim. Acta*, 1984, **86**, 173.
26 G. Matsubayashi, Y. Yamaguchi and T. Tanaka, *J. Chem. Soc.*, *Dalton Trans.*, 1988, 2216.
27 (*a*) R. Rafikov, J. Weinstein, M. Mel'nikov and N. Zheligovskaya, unpublished work; (*b*) *Absorption Spectra in Ultraviolet and Visible Region*, ed. L. Lang, Akademiai, Budapest, 1971, vol. 15, pp. 127–128.
28 R. M. Wallac and S. M. Katz, *J. Phys. Chem.*, 1964, **68**, 3890.
29 Y. Zhang, K. D. Ley and K. S. Schanze, *Inorg. Chem.*, 1996, **35**, 7102.
30 K. Base and M. W. Grinstaff, *Inorg. Chem.*, 1998, **37**, 1432.
31 D. J. Stufkens, T. L. Snoeck and A. B. P. Lever, *Inorg. Chem.*, 1988, **27**, 953.

Received 29*th April* 1998; *Paper* 8/03225D